**Advances in Robotics Research**, *Vol. 1, No. 2 (2014) 141-154*
DOI: http://dx.doi.org/10.12989/arr.2014.1.2.141 

# Deformation analysis of a 3-DOF parallel manipulator with one or two additional branches

Xiaolei Chen[1,2], Jun Wu[*1,2], Guang Yu[1,2] and Liping Wang[1,2]

[1]*Institute of Manufacturing Engineering, Department of Mechanical Engineering, Tsinghua University, Beijing 100084, China*
[2]*Beijing Key Lab of Precision/Ultra-precision Manufacturing Equipments and Control, Beijing 100084, China*

*(Received October 7, 2013, Revised December 7, 2013, Accepted December 22, 2013)*

**Abstract.** Redundant parallel manipulators have some advantages over the nonredundant parallel manipulators. It is important to determine how many additional branches should be introduced. This paper studies whether one or two additional branches should be added to a 3-DOF parallel manipulator by comparing the flexible deformation of a 3-DOF parallel manipulator with one additional branch and that with two additional branches. The kinematic and dynamic models of the redundant parallel manipulator are derived and the flexible deformation is investigated. The flexible deformation of the manipulators with one additional branch and two branches is simulated and compared. This paper is helpful for designers to design a redundantly actuated parallel manipulator.

**Keywords:** parallel manipulator; flexible deformation; principal of virtual work; dynamics

## 1. Introduction

Parallel manipulators have attracted much attention due to its advantages comparing with serial manipulators, such as high payload to weight ratio, better dynamic performance and higher stiffness. However, parallel manipulators suffer from some drawbacks, including small workspace as well as lots of singular configurations in the workspace. It is believed that redundant actuation is an approach to improve the kinematic and dynamic properties of parallel manipulators (Buttolo and Hannaford 1995, Wang and Gosselin 2004, Nokleby *et al.* 2005). The presence of one or more redundant actuated chains in the structure has many advantages for parallel manipulators such as avoiding kinematic singularities, enlarging load capability and improving dynamic characteristics (Merlet 1996, Nahon and Angeles 1992). Redundantly actuated parallel manipulators have been applied to multi-finger robotic hands (Yi *et al.* 1999) and parallel machining centers (Wu *et al.* 2009, Kim *et al.* 2001).

Stiffness is one of the most important performances of parallel manipulators, particularly for those which are used as machine tools, since higher stiffness allows higher machining speeds and feeds while providing the desired precision, surface finish, and tool life (Gao *et al.* 2010, Zhang *et*

[*]Corresponding author, Ph.D., E-mail: jhwu@mail.tsinghua.edu.cn

**Copyright © 2014 Techno-Press, Ltd.**
 ISSN: 2287-4976 (Print), 2287-4984 (Online)

*al.* 2010, Hao and Kong 2012, Yun and Li 2012). Many publications have contributed to the stiffness modeling and evaluation of the stiffness of a parallel manipulator in the usable workspace. Gosselin (1990) and Svinin (2001) investigated the stiffness of Stewart platform and the mapping between the driving force and the platform deformation based on the Jacobian matrix. Ceccarelli (2002) established a stiffness model of the 3-DOF CaPaMan parallel manipulator by taking into account the kinematic and static features of the three legs. The commercial finite element software, for example ANSYS, ABAQUS and NASTRAN are also used to investigate the stiffness of a machine tool (Huang and Lee 2001).These methods are extended to redundantly actuated parallel manipulators (Zhao and Gao 2009, Thanh *et al.* 2012). However, most of the work focuses on the static stiffness of parallel manipulators. In motion, the moving parts of a parallel manipulator with lowest stiffness maybe have larger flexible deformation under the act of inertial forces. The flexible deformation is different with the deformation computed from the static stiffness model. Moreover, little work has been done on the deformation comparison of the redundant parallel manipulators with one additional branch and those with more than one additional branch.

In this paper, the flexible deformation of a 3-DOF parallel manipulator with one additional branch or two additional branches in motion is investigated. The dynamic model is derived by taking the flexible deformation of both the link and the joint into account. The flexible deformation of the parallel manipulator with one additional branch is compared with that with two additional branches. This paper can provide guidance for designer to determine how many additional branches should be added.

## 2. Kinematic analysis

### *2.1 Position analysis*

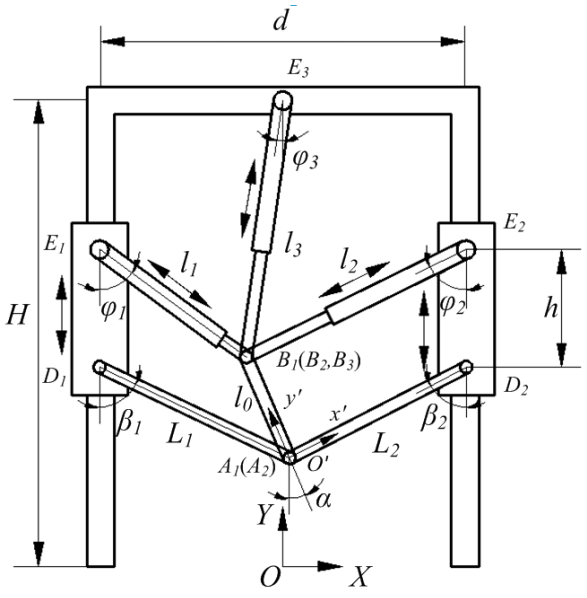


Fig. 1 The kinematic model of the 3-DOF parallel manipulator

Fig. 1 shows the kinematic model of a 3-DOF parallel manipulator. In fact, the parallel manipulator has a 3-DOF motion capability without links $B_1E_1$ and $B_3E_3$. Links $B_1E_1$ and $B_3E_3$ are introduced to improve the manipulator performance. In this paper, one additional link denotes links $B_1E_1$ and two additional links denote links $B_1E_1$ and $B_3E_3$. A base coordinate system $OXY$ is attached to the base in the middle of the two columns. A moving coordinate system $O'x'y'$ is attached to end point $A_i$ of the mobile platform. The position vector of point $A_i$ with respect to $OXY$ is $\boldsymbol{r}_{A_i} = [x, y]^T$, and the rotational angle of the mobile platform is $\alpha$. $l_0$ is the length of the mobile platform.

The position vector of point $B_i$ with respect to $OXY$ can be expressed as

$$\boldsymbol{r}_{B_i} = [x_{B_i}, y_{B_i}]^T = \boldsymbol{r}_{A_i} + \boldsymbol{R}\boldsymbol{r}'_{B_i}, i = 1,2,3 \tag{1}$$

where $\boldsymbol{r}'_{B_i} = [x'_{B_i}, y'_{B_i}]^T = [0, l_0]$ is the position vector of $B_i$ with respect to $O'x'y'$, and $\boldsymbol{R} = \begin{bmatrix} \cos\alpha & -\sin\alpha \\ \sin\alpha & \cos\alpha \end{bmatrix}$ is the rotation matrix from $O'x'y'$ to $OXY$.

The constraint equation of link $A_iD_i$ and link $B_iE_i$ can be written as

$$\boldsymbol{r}_{D_i} = \boldsymbol{r}_{A_i} + L_i\boldsymbol{n}_i, i = 1,2 \tag{2}$$

$$\boldsymbol{r}_{E_i} = \boldsymbol{r}_{B_i} + l_i\boldsymbol{s}_i, i = 1,2,3 \tag{3}$$

where $L_i$ and $l_i$ are the length of link $A_iD_i$ and link $B_iE_i$, $\boldsymbol{n}_i$ and $\boldsymbol{s}_i$ are the unit vectors of link $A_iD_i$ and link $B_iE_i$, and $\boldsymbol{r}_{Di}$ and $\boldsymbol{r}_{Ei}$ are the position vectors of point $D_i$ and point $E_i$, respectively.

By taking the 2-norm of both sides of Eqs. (2) and (3), the position of the slider $D_iE_i$ and the length of link $B_iE_i$ can be written as

$$q_1 = y + L_1\cos\beta_1 \tag{4}$$

$$q_2 = y + L_2\cos\beta_2 \tag{5}$$

$$l_1 = \sqrt{\left(x - l_0\sin\alpha + \frac{d}{2}\right)^2 - \left(y + l_0\cos\alpha - q_1 - h\right)^2} \tag{6}$$

$$l_2 = \sqrt{\left(x - l_0\sin\alpha - \frac{d}{2}\right)^2 - \left(y + l_0\cos\alpha - q_2 - h\right)^2} \tag{7}$$

$$l_3 = \sqrt{\left(x - l_0\sin\alpha\right)^2 - \left(y + l_0\cos\alpha - H\right)^2} \tag{8}$$

where $q_1$ and $q_2$ are the $Y$ positions of the sliders $D_1E_1$ and $D_2E_2$, $d$ is the length between two columns, $h$ is the length of the slider and $H$ is the height of the column. $\beta_i$ is the angle between link $A_iD_i$ and the column.

### *2.2 Velocity analysis*

Taking the derivative of Eq. (1) with respect to time, the velocity of point $B_i$ can be obtained as

$$\dot{\boldsymbol{r}}_{B_i} = [\dot{x}_{B_i}, \dot{y}_{B_i}]^T = \dot{\boldsymbol{r}}_{A_i} + \dot{\alpha}\boldsymbol{E}\boldsymbol{R}\boldsymbol{r}'_{B_i}, i = 1,2,3 \tag{9}$$

where $\dot{\boldsymbol{r}}_{A_i} = [\dot{x}, \dot{y}]^T$ is the velocity of point $A_i$, $\dot{\alpha}$ is the angular velocity of the mobile platform, and $\boldsymbol{E} = \begin{bmatrix} 0 & -1 \\ 1 & 0 \end{bmatrix}$.

Taking the derivative of Eqs. (4) and (5) with respect to time, the velocity of slider can be expressed as

$$\dot{q}_i = \dot{y} - L_i\dot{\beta}_i \sin\beta_i, i = 1,2 \tag{10}$$

where $\dot{\beta}_i$ is the angular velocity of link $A_iD_i$,

$$\dot{\beta}_i = \frac{\dot{x}}{L_i \cos\beta_i}, i = 1,2 \tag{11}$$

Taking the derivative of Eqs. (6)-(8) with respect to time yields

$$\dot{l}_i = \dot{x}_{B_i}\sin\varphi_i + \left(\dot{q}_i - \dot{y}_{B_i}\right)\cos\varphi_i, i = 1,2,3 \tag{12}$$

where $\dot{l}_i$ is the stretch velocity of link $B_iE_i$ and $\varphi_i$ is the angle between link $B_iE_i$ and $Y$ axis. Similarly the angular velocity of link $B_iE_i$ can be written as

$$\dot{\varphi}_i = \frac{\dot{x}\cos\varphi_i + (\dot{y} - \dot{q}_i)\sin\varphi_i}{l_i}, i = 1,2,3 \tag{13}$$

### *2.3 Jacobian matrix*

It is well accepted that the condition number of Jacobian matrix is a local performance index for evaluating the velocity, accuracy and rigidity mapping characteristics between the joint variables and the moving platform. The Jacobian matrix can be written as

$$\dot{\boldsymbol{q}} = \boldsymbol{J} \cdot \dot{\boldsymbol{p}} \tag{14}$$

where $\dot{\boldsymbol{q}} = \begin{bmatrix} \dot{q}_1 & \dot{q}_2 & \dot{l}_1 & \dot{l}_2 & \dot{l}_3 \end{bmatrix}^T$, and $\dot{\boldsymbol{p}} = \begin{bmatrix} \dot{x} & \dot{y} & \dot{\alpha} \end{bmatrix}^T$.

Based on Eqs. (10)-(13), the Jacobian matrix can be formulated as

$$\boldsymbol{J} = \begin{bmatrix} \boldsymbol{J}_1 & \boldsymbol{J}_2 & \boldsymbol{J}_3 & \boldsymbol{J}_4 & \boldsymbol{J}_5 \end{bmatrix} = \begin{bmatrix} -\tan\beta_1 & -\tan\beta_2 & J_{13} & J_{14} & J_{15} \\ 1 & 1 & 0 & 0 & 0 \\ 0 & 0 & J_{33} & J_{34} & J_{35} \end{bmatrix}^T \tag{15}$$

where

$$J_{13} = \sin\varphi_1 - \cos\varphi_1 - \tan\beta_1\cos\varphi_1,$$

$$J_{33} = -l_0\cos\alpha\sin\varphi_1 + l_0\sin\alpha\cos\varphi_1,$$
$$J_{14} = \sin\varphi_2 - \cos\varphi_2 - \tan\beta_2\cos\varphi_2,$$
$$J_{34} = -l_0\cos\alpha\sin\varphi_2 + l_0\sin\alpha\cos\varphi_2,$$
$$J_{15} = \sin\varphi_3 - \cos\varphi_3,$$
$$J_{35} = -l_0\cos\alpha\sin\varphi_3 + l_0\sin\alpha\cos\varphi_3.$$

In this paper, the principle of virtual work is utilized to derive the dynamic model, and the link Jacobian matrices used in the dynamic model should be derived. For slider, taking point $E_i$ as pivotal point, the link Jacobian matrices related to the linear velocity and angular velocity can be expressed as

$$\boldsymbol{H}_{1i} = \begin{bmatrix} 0 & 1 \end{bmatrix} \cdot \boldsymbol{J}_1, i = 1,2 \tag{16}$$

$$\boldsymbol{G}_{1i} = 0, i = 1,2 \tag{17}$$

For link $A_iD_i$, taking point $D_i$ as pivotal point, the link Jacobian matrices related to the linear velocity and angular velocity can be expressed as

$$\boldsymbol{H}_{2i} = \boldsymbol{H}_{1i}, i = 1,2 \tag{18}$$

$$\boldsymbol{G}_{2i} = [\frac{1}{L_i\cos\beta_i}, 0] \cdot ([\boldsymbol{e}_1, \boldsymbol{e}_2]^T + \boldsymbol{E}\boldsymbol{R}\boldsymbol{r}_{A_i}^{'}\boldsymbol{e}_3^T), i = 1,2 \tag{19}$$

where $\boldsymbol{e}_1 = \begin{bmatrix} 1 & 0 & 0 \end{bmatrix}$, $\boldsymbol{e}_2 = \begin{bmatrix} 0 & 1 & 0 \end{bmatrix}$ and $\boldsymbol{e}_3 = \begin{bmatrix} 0 & 0 & 1 \end{bmatrix}$ are the unit vectors.

For upper part of link $B_iE_i$, taking point $E_i$ as pivotal point, the link Jacobian matrices related to the linear velocity and angular velocity can be written as

$$\boldsymbol{H}_{3i} = \begin{bmatrix} 0,1 \end{bmatrix}^T \cdot \boldsymbol{J}_{\boldsymbol{i}}, i = 1,2,3 \tag{20}$$

$$\boldsymbol{G}_{3i} = [\frac{\cos\varphi_i}{l_i}, \frac{\sin\varphi_i}{l_i}] \cdot ([\boldsymbol{e}_1, \boldsymbol{e}_2]^T + \boldsymbol{E}\boldsymbol{R}\boldsymbol{r}_{B_i}^{'}\boldsymbol{e}_3^T) - \frac{\sin\varphi_i}{l_i} \cdot \boldsymbol{J}_{i+2}, i = 1,2,3 \tag{21}$$

For lower part of link $B_iE_i$, taking point $B_i$ as pivotal point, the link Jacobian matrices related to the linear velocity and angular velocity can be written as

$$\boldsymbol{H}_{4i} = \begin{bmatrix} \boldsymbol{e}_1, \boldsymbol{e}_2 \end{bmatrix}^T + \boldsymbol{E}\boldsymbol{R}\boldsymbol{r}_{B_i}^{'}\boldsymbol{e}_3^T, i = 1,2,3 \tag{22}$$

$$\boldsymbol{G}_{4i} = \boldsymbol{G}_{3i}, i = 1,2,3 \tag{23}$$

For the mobile platform, the link Jacobian matrices related to the linear velocity and angular velocity can be expressed as

$$\boldsymbol{H}_N = \begin{bmatrix} \boldsymbol{e}_1, \boldsymbol{e}_2 \end{bmatrix}^T \tag{24}$$

$$\boldsymbol{G}_N = \boldsymbol{e}_3^T \tag{25}$$

## 3. Dynamic analysis

### 3.1 Acceleration analysis

Taking the derivative of Eq. (9) with respect to time, the acceleration of point $B_i$ can be written as

$$\ddot{\boldsymbol{r}}_{B_i} = [\ddot{x}_{B_i}, \ddot{y}_{B_i}]^T = \ddot{\boldsymbol{r}}_{A_i} + \ddot{\alpha}\boldsymbol{E}\boldsymbol{R}\boldsymbol{r}'_{B_i} - \dot{\alpha}^2\boldsymbol{E}\boldsymbol{R}\boldsymbol{r}'_{B_i}, i = 1,2,3 \tag{26}$$

where $\ddot{\boldsymbol{r}}_{A_i} = \left[\ddot{x}, \ddot{y}\right]^T$ is the acceleration of point $A_i$, and $\ddot{\alpha}$ is the angular acceleration of the mobile platform.

Taking the derivative of Eq. (10) with respect to time, the acceleration of slider can be written as

$$\ddot{q}_i = \ddot{y} - L_i\ddot{\beta}_i \sin\beta_i - L_i\dot{\beta}_i \cos\dot{\beta}_i, i = 1,2 \tag{27}$$

where $\ddot{\beta}_i$ is the angular acceleration of link $A_iD_i$.

Taking the derivative of Eq. (12) with respect to time yields

$$\ddot{l}_i = \ddot{x}_{B_i} \sin\varphi_i + \dot{x}_{B_i}\dot{\varphi}_i \cos\varphi_i + \left(\ddot{q}_2 - \ddot{y}_{B_i}\right)\cos\varphi_2 - \left(\dot{q}_i - \dot{y}_{B_i}\right)\dot{\varphi}_i \sin\varphi_i, i = 1,2,3 \tag{28}$$

where $\ddot{l}_i$ is the stretch acceleration of link $B_iE_i$.

Taking the derivative of Eqs. (11) and (13) with respect to time yields

$$\ddot{\beta}_i = \frac{\ddot{x}L_i\cos\beta_i + \dot{x}\tan\beta_i}{L_i^2\cos^2\beta_i}, i = 1,2 \tag{29}$$

$$\ddot{\varphi}_i = \frac{\ddot{x}\cos\varphi_i - \dot{x}\dot{\varphi}_i \sin\varphi_i + (\ddot{y} - \ddot{q}_i)\sin\varphi_i + (\dot{y} - \dot{q}_i)\dot{\varphi}_i \cos\varphi_i - \dot{\varphi}_i\dot{l}_i}{l_i}, i = 1,2,3 \tag{30}$$

where $\ddot{\varphi}_i$ is the stretch acceleration of link $B_iE_i$.

Then points $D_i$ and $E_i$ have the same acceleration only in the vertical direction which is equal to that of the sliders, thus the accelerations of points $D_i$ and $E_i$ can be written as

$$\boldsymbol{a}_{D_i} = \boldsymbol{a}_{E_i} = \left[0,1\right]^T \ddot{q}_i, i = 1,2 \tag{31}$$

### 3.2 Inertial force and moment

The inertial forces and moments about those pivotal points chosen in Section 3.1 are needed in the dynamic modeling based on the principle of virtual work, and the Newton-Euler approach is used to find inertial forces and moments. Supposing that the mass centers of moving parts are located in the middle of the links, the inertial force and moment of slider about pivotal point $E_i$ can be written as

$$\boldsymbol{F}_{1i} = -m_{1i}\left(\boldsymbol{a}_{E_i} - \boldsymbol{g}\right), i = 1,2 \tag{32}$$

$$\boldsymbol{M}_{1i} = 0, i = 1,2 \tag{33}$$

where $m_{1i}$ is the mass of slider, $\boldsymbol{g}=\begin{bmatrix}0 & -g\end{bmatrix}$ is the acceleration of gravity, and $g=9.8m/s^2$.

The inertial force and moment of link $A_iD_i$ about pivotal point $D_i$ can be written as

$$\boldsymbol{F}_{2i}=-m_{2i}\left(\boldsymbol{a}_{D_i}+\frac{\ddot{\beta}_i L_i \boldsymbol{E}\boldsymbol{n}_i}{2}-\frac{\dot{\beta}_i^2 L_i \boldsymbol{n}_i}{2}-\boldsymbol{g}\right), i=1,2 \tag{34}$$

$$\boldsymbol{M}_{2i}=-I_{2i}\ddot{\beta}_i+\frac{m_{2i}L_i\boldsymbol{n}_i\boldsymbol{E}\left(\boldsymbol{a}_{D_i}-\boldsymbol{g}\right)}{2}, i=1,2 \tag{35}$$

where $m_{2i}$ is the mass of link $A_iD_i$, and $I_{2i}$ is the moment of inertia of link $A_iD_i$ about point $D_i$.

The inertial force and moment of upper part of link $B_iE_i$ about pivotal point $E_i$ can be written as

$$\boldsymbol{F}_{3i}=-m_{3i}\left(\boldsymbol{a}_{E_i}+\frac{\ddot{\varphi}_i l_{i1}\boldsymbol{E}\boldsymbol{s}_i}{2}-\frac{\dot{\varphi}_i^2 l_{i1}\boldsymbol{s}_i}{2}-\boldsymbol{g}\right), i=1,2,3 \tag{36}$$

$$\boldsymbol{M}_{3i}=-I_{3i}\ddot{\varphi}_i+\frac{m_{3i}l_{i1}\boldsymbol{s}_i\boldsymbol{E}\left(\boldsymbol{a}_{E_i}-\boldsymbol{g}\right)}{2}, i=1,2,3 \tag{37}$$

where $m_{3i}$ is the mass of upper part of link $B_iE_i$, and $I_{3i}$ is the moment of inertia of upper part of link $B_iE_i$ about point $E_i$, and $l_{i1}$ is the length of upper part of link $B_iE_i$.

The inertial force and moment of lower part of link $B_iE_i$ about pivotal point $B_i$ can be written as

$$\boldsymbol{F}_{4i}=-m_{4i}\left(\boldsymbol{a}_{B_i}-\frac{\ddot{\varphi}_i l_{i2}\boldsymbol{E}\boldsymbol{s}_i}{2}+\frac{\dot{\varphi}_i^2 l_{i2}\boldsymbol{s}_i}{2}-\boldsymbol{g}\right), i=1,2,3 \tag{38}$$

$$\boldsymbol{M}_{4i}=-I_{4i}\ddot{\varphi}_i-\frac{m_{4i}l_{i2}\boldsymbol{s}_i\boldsymbol{E}\left(\boldsymbol{a}_{B_i}-\boldsymbol{g}\right)}{2}, i=1,2,3 \tag{39}$$

where $m_{4i}$ is the mass of lower part of link $B_iE_i$, $I_{4i}$ is the moment of inertia of upper part of link $B_iE_i$ about point $B_i$, and $l_{i2}$ is the length of lower part of link $B_iE_i$.

The inertial force and moment of mobile platform can be written as

$$\boldsymbol{F}_N=-m_N\left(\boldsymbol{a}_{A_i}-\frac{\ddot{\alpha}\boldsymbol{E}\boldsymbol{R}\boldsymbol{r}'_{B_i}}{2}+\frac{\dot{\alpha}_i^2\boldsymbol{R}\boldsymbol{r}'_{B_i}}{2}-\boldsymbol{g}\right) \tag{40}$$

$$\boldsymbol{M}_N=-I_N\ddot{\alpha}-\frac{m_N\boldsymbol{R}\boldsymbol{r}'_{B_i}\boldsymbol{E}\left(\boldsymbol{a}_{A_i}-\boldsymbol{g}\right)}{2} \tag{41}$$

where $m_N$ is the mass of mobile platform and $I_N$ is the moment of inertia of the mobile platform.

### 3.3 Dynamic equation

Based on the principle of virtual work, it can be obtained that

$$\boldsymbol{\tau}^T \cdot \Delta \boldsymbol{q} + \sum_1^n \boldsymbol{R}_i^T \cdot \boldsymbol{v}_i + \sum_1^n \boldsymbol{T}_i^T \cdot \boldsymbol{\omega}_i = 0 \tag{42}$$

where $\boldsymbol{R}_i$ and $\boldsymbol{T}_i$ are the force matrix and moment matrix of moving part, $\boldsymbol{v}_i$ and $\boldsymbol{\omega}_i$ are the velocity and angular velocity of moving part, respectively. $\Delta \boldsymbol{q}$ is the virtual displacement and $\boldsymbol{\tau}$ is the driving force of actuators, and $\boldsymbol{\tau} = \begin{bmatrix} \tau_1 & \tau_2 & \tau_3 & \tau_4 & \tau_5 \end{bmatrix}^T$.

Substituting the link Jacobian matrices related to the linear velocity and angular velocity into Eq. (42) leads to

$$\boldsymbol{J}^T \cdot \boldsymbol{\tau} + \sum_{j=1}^{2} \sum_{i=1}^{4} \begin{bmatrix} \boldsymbol{H}_{ji}^T, \boldsymbol{G}_{ji}^T \end{bmatrix} \cdot \begin{bmatrix} \boldsymbol{F}_{ji} \\ \boldsymbol{M}_{ji} \end{bmatrix} + \sum_{j=3}^{4} \begin{bmatrix} \boldsymbol{H}_{j3}^T, \boldsymbol{G}_{j3}^T \end{bmatrix} \cdot \begin{bmatrix} \boldsymbol{F}_{j3} \\ \boldsymbol{M}_{j3} \end{bmatrix} + \begin{bmatrix} \boldsymbol{H}_N^T, \boldsymbol{G}_N^T \end{bmatrix} \cdot \begin{bmatrix} \boldsymbol{F}_N \\ \boldsymbol{M}_N \end{bmatrix} = 0 \tag{43}$$

### 3.4 Deformation analysis

In the deformation analysis, the axial deformation of links is considered. The deformation of link $A_iD_i$ is much smaller than that of link $B_iE_i$, thus the deformation of link $B_iE_i$ is mainly considered in deformation analysis and the deformation of link $A_iD_i$ is neglected. Thus only the angular deformation of the mobile platform should be considered. The relationship between the deformation of link $B_iE_i$ and the angular deformation of mobile platform can be described as

$$\begin{bmatrix} u_1 \\ u_2 \\ u_3 \end{bmatrix} = \boldsymbol{U} d\alpha \tag{44}$$

where $\boldsymbol{U} = l_0 \cdot \begin{bmatrix} \sin\varphi_1 \cos\alpha + \cos\varphi_1 \sin\alpha \\ \sin\varphi_2 \cos\alpha + \cos\varphi_2 \sin\alpha \\ \sin\varphi_3 \cos\alpha + \cos\varphi_3 \sin\alpha \end{bmatrix}$, $d\alpha$ is the angular deformation of mobile platform, and $u_i$ is the deformations of link $B_iE_i$ and can be expressed as

$$u_i = -\tau_{i+2} \frac{l_i}{E_0 S_A} - m_{3i} l_i \boldsymbol{s}_i \left( \boldsymbol{g} - \boldsymbol{a}_{l_i}^u \right) \frac{l_{i1}}{2E_0 S_A} + m_{4i} l_i \boldsymbol{s}_i \left( \boldsymbol{g} - \boldsymbol{a}_{l_i}^l \right) \frac{l_{i2}}{2E_0 S_A}, i = 1,2,3 \tag{45}$$

where $E_0$ is the Young's modulus of link $B_iE_i$, and $S_A$ is the sectional area of link $B_iE_i$. $\boldsymbol{a}_{l_i}^u$ and $\boldsymbol{a}_{l_i}^l$ are the accelerations of mass center of upper part and lower part of link $B_iE_i$, respectively. $\boldsymbol{a}_{l_i}^u$ and $\boldsymbol{a}_{l_i}^l$ can be expressed as

$$\boldsymbol{a}_{l_i}^u = a_{E_i} + s_{3i} \ddot{\varphi} E \left[ \sin\varphi_i, -\cos\varphi_i \right]^T - s_{3i} \dot{\varphi}_i^2 \left[ \sin\varphi_i, -\cos\varphi_i \right]^T, i = 1,2,3 \tag{46}$$

$$\boldsymbol{a}_{l_i}^l = a_{B_i} - s_{4i} \ddot{\varphi} E \left[ \sin\varphi_i, -\cos\varphi_i \right]^T + s_{4i} \dot{\varphi}_i^2 \left[ \sin\varphi_i, -\cos\varphi_i \right]^T, i = 1,2,3 \tag{47}$$

where $s_{3i}$ is the distance from point $B_i$ to the mass center of upper part of link $B_iE_i$ and $s_{4i}$ is

the distance from point $E_i$ to the mass center of lower part of link $B_iE_i$.

The deformation of the joint between slider and link can be written as

$$u_i^J = -\frac{m_{3i}l_i\boldsymbol{s}_i\left(\boldsymbol{g}-\boldsymbol{a}_{l_i}^u\right)+m_{4i}l_i\boldsymbol{s}_i\left(\boldsymbol{g}-\boldsymbol{a}_{l_i}^l\right)}{k}, i=1,2,3 \tag{48}$$

where $k$ is the stiffness of joint between slider and link.

Based on Eqs. (44)-(48), the total deformation can be rewritten as

$$\begin{bmatrix} u_1' \\ u_2' \\ u_3' \end{bmatrix} = \boldsymbol{U}d\alpha \tag{49}$$

where $u_i' = u_i + u_i^J$.

## 4. Numerical simulations

### *4.1 Simulation without payload*

Both the flexible deformation of the link and that of the joint are taken into account. In simulation, the end point $A_i$ of the mobile platform moves from point (-0.4 m, 0.4 m) to point (0.4 m, 0.4 m) with respect to coordinate system $OXY$, while the angle $\alpha$ varies from $-\pi/10$ to $\pi/10$. The maximum velocity of point $A_i$ in the motion is 1.2 m/s, and the "S" speed strategy (Wu et al. 2007) is used to plan the trajectory. The geometrical and inertial parameters are shown in Table 1.

The deformation of mobile platform of the manipulators with one additional link and two links is shown in Fig. 2, and the driving forces are shown in Figs. 3 and 4. One may see that the

Table 1Geometrical and inertial parameters

| Parameters | Values | Parameters | Values |
|---|---|---|---|
| $l_0$ | 0.25 m | $I_{41}, I_{42}, I_{43}$ | 4.27 kg m$^2$ |
| $L_1, L_2$ | 1.15 m | $I_N$ | 10.12 kg m$^2$ |
| $h$ | 0.25 m | $m_{11}, m_{12}$ | 120 kg |
| $H$ | 3 m | $m_{21}, m_{22}$ | 220 kg |
| $d$ | 1.17 m | $m_{31}, m_{32}, m_{33}$ | 60 kg |
| $l_{11}, l_{21}, l_{31}$ | 1 m | $m_{41}, m_{42}, m_{43}$ | 20 kg |
| $l_{12}, l_{22}, l_{32}$ | 0.5 m | $m_N$ | 150 kg |
| $I_{21}, I_{22}$ | 105.6 kg m$^2$ | $E_0$ | $2.1\times10^{11}$ pa |
| $I_{31}, I_{32}, I_{33}$ | 7.2 kg m$^2$ | $S_A$ | $1.5\times10^{-3}$ m$^2$ |

deformation of the mobile platform of the manipulator with two additional links is similar to that of the manipulator with one additional link. Furthermore, the driving forces of the manipulator with two additional links are also similar to those of the manipulator with one additional link.

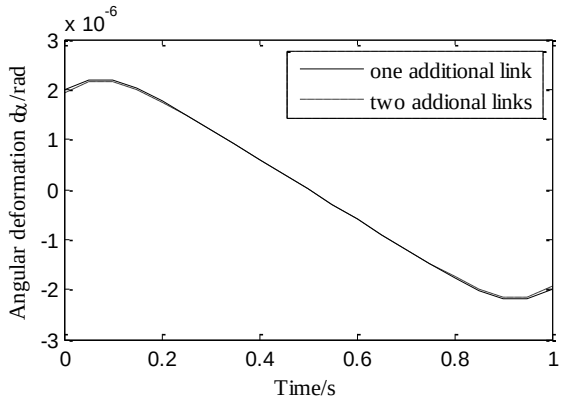


Fig. 2 Angular deformation considering the link and joint deformation

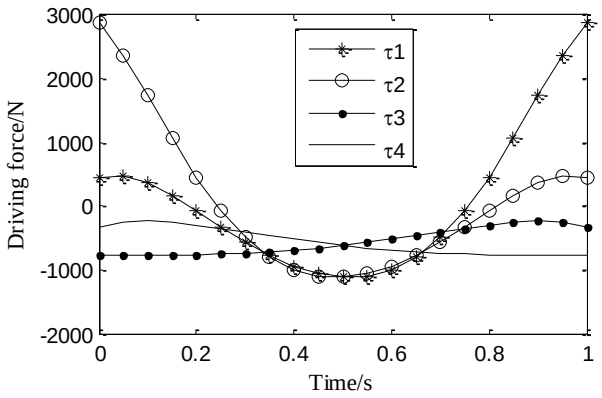


Fig. 3 Driving force considering the link and joint (one additional link)

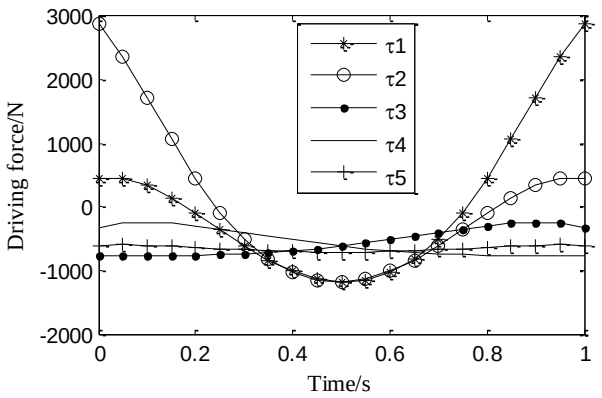


Fig. 4 Driving force considering the link and joint (two additional links)

### *4.2 Simulation with payload*

From the above deformation simulations, it can be concluded that the deformation of the manipulator with two additional links is similar to that of the other with one additional link. Since the payload can be evaluated by the external force acting on the mobile platform that a manipulator can support, the payload is considered to simulate the deformation of the manipulator with one or two additional links. It is assumed that the payload acting on the mobile platform is an external force $\boldsymbol{F}_{ext}$. Based on the principle of virtual work, Eq. (43) can be rewritten as

$$\boldsymbol{J}^T \cdot \boldsymbol{\tau} + \sum_{j=1}^{2}\sum_{i=1}^{4}\left[\boldsymbol{H}_{ji}^T, \boldsymbol{G}_{ji}^T\right] \cdot \begin{bmatrix} \boldsymbol{F}_{ji} \\ \boldsymbol{M}_{ji} \end{bmatrix} + \sum_{j=3}^{4}\left[\boldsymbol{H}_{j3}^T, \boldsymbol{G}_{j3}^T\right] \cdot \begin{bmatrix} \boldsymbol{F}_{j3} \\ \boldsymbol{M}_{j3} \end{bmatrix} + \left[\boldsymbol{H}_N^T, \boldsymbol{G}_N^T\right] \cdot \begin{bmatrix} \boldsymbol{F}_N \\ \boldsymbol{M}_N \end{bmatrix} + \boldsymbol{F}_{ext} = 0 \tag{50}$$

In the follow simulations, it is supposed that the external force acts on the mobile platform along the horizontal direction. With the motion trajectory and parameters shown in Section 4.1, the angular deformation and the maximum payload considering the external force and the deformation of link $B_iE_i$ and the joint are shown in Figs. 5 and 6, and the driving forces are shown in Figs. 7 and 8.

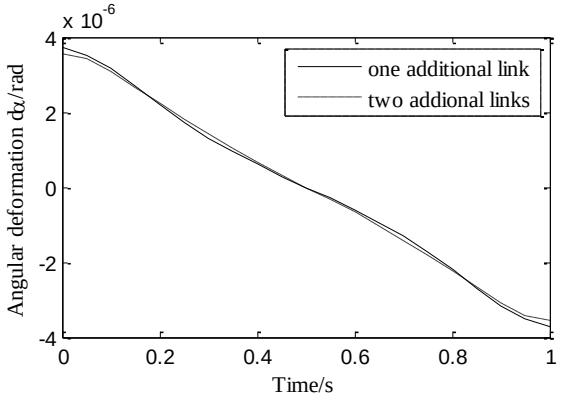


Fig. 5 Angular deformation considering the payload

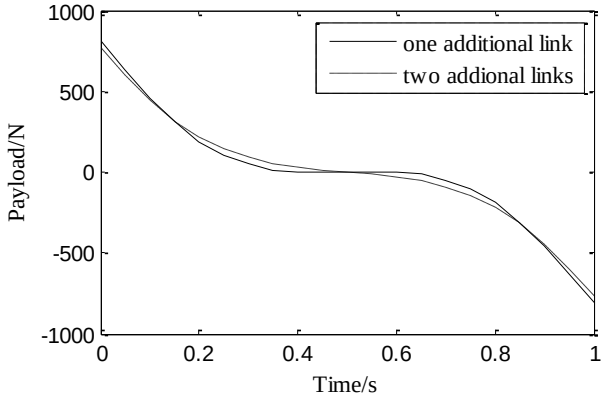


Fig. 6 Payload in the horizontal direction

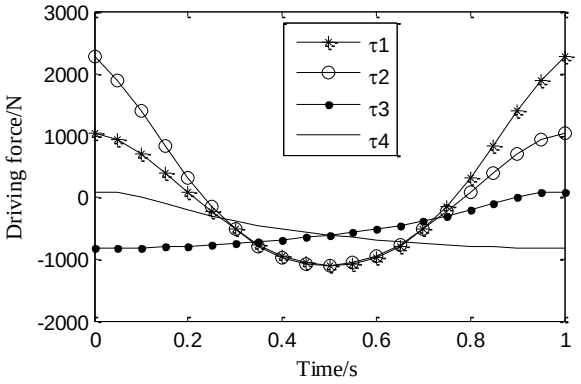


Fig. 7 Driving force considering the payload (one additional link)

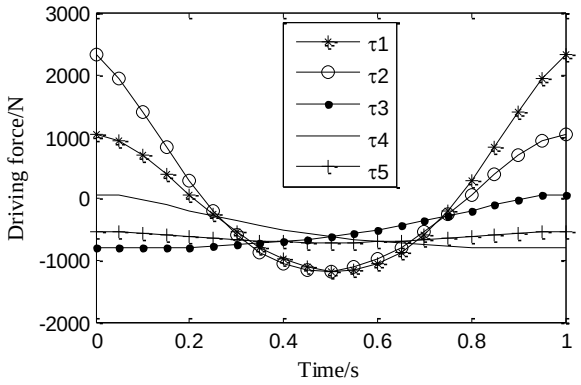


Fig. 8 Driving force considering the payload (two additional links)

It can be concluded that the angular deformation considering the payload is larger than that without considering the payload. There is a little difference between the deformation of the manipulator with one additional link and that with two additional links. From Fig. 6, it can be seen that the payload of the manipulator with one additional link is similar to that with two additional links. With payload, the driving forces of the manipulator with two additional links are similar to those of the manipulator with one additional link. Considering the control and manufacturing cost, it is better to design the redundant parallel manipulator with one additional link.

## 5. Conclusions

The flexible deformation of a 3-DOF parallel manipulator with one or two additional branches has been investigated. Based on the principle of virtue work, the dynamic model is derived and the flexible deformation of both joint and link is considered. Without payload, the flexible deformation of the manipulator with one additional link $B_1E_1$ is similar to that of the manipulator with two additional links $B_1E_1$ and $B_3E_3$. The flexible deformation of the manipulator with payload is greater than that without payload. Considering the manufacturing cost and control

problem, it is better to develop the parallel manipulator with one additional link $B_1E_1$. The paper is useful for the designer to design a redundant parallel manipulator.

## Acknowledgements

This work is supported by the National Natural Science Foundation of China (Grant No. 51105225, 51225503 and 51375210), a foundation for the author of national excellent doctoral dissertation of PR China (201137), and the Science and Technology Major Project-Advanced NC Machine Tools & Basic Manufacturing Equipments (2013ZX04004021, 2014ZX04002051).

## References

Buttolo, P. and Hannaford, B. (1995), "Advantages of actuation redundancy for the design of haptic displays", *Proceedings of ASME Int. Mechanical Engineering Congress and Exposition*, San Francisco, CA, USA, November.

Ceccarelli, M. and Carbone, G. (2002), "A stiffness analysis for CaPaman (Cassino Parallel Manipulator)", *Mech. Mach. Theory*, **37**(5), 427-439.

Gao, Z., Zhang, D., Hu, X.L. and Ge, Y.J. (2010), "Design, analysis, and stiffness optimization of a three degree of freedom parallel manipulator", *Robotica*, **28**(3), 349-357.

Gosselin, C.M. (1990), "Stiffness mapping for parallel manipulators", *IEEE Trans. Rob. Autom.*, **6**(3), 377-382.

Hao, G.B. and Kong, X.W. (2012), "A novel large-range XY compliant parallel manipulator with enhanced out-of-plane stiffness", *J. Mech. Des.*, **134**(6), 061009-1-061009-9.

Huang, D.T.Y. and Lee, J.J. (2001), "On obtaining machine tool stiffness by CAE techniques", *Int. J. Mach. Tools Manuf.*, **41**(8), 1149-1163.

Kim, J., Park, F.C., Ryu, S.J., Kim, J., Hwang, J.C., Park, C. and Iurascu, C.C. (2001), "Design and analysis of a redundantly actuated parallel mechanism for rapid machining", *IEEE Trans. Rob. Autom.*, **17**(4), 423-434.

Merlet, J.P. (1996), "Redundant parallel manipulators", *Lab. Rob. Autom.*, **8**(1), 17-24.

Nahon, M. and Angeles, J. (1992), "Real-time force optimization in parallel kinematic chains under inequality constraints", *IEEE Trans. Rob. Autom.*, **8**(4), 439-450.

Nokleby, S.B., Fisher, R., Podhorodeski, R.P. and Firmani, F. (2005), "Force capabilities of redundantly-actuated parallel manipulators", *Mech. Mach. Theory*, **40**(5), 578-599.

Svinin, M.M., Hosoe, S. and Uchiyana, M. (2001), "On the stiffness and stability of Gough-Stewart platforms", *IEEE Int. Conf. on Robotics and Automation*, Seoul, Korea, May.

Thanh, T.D., Kotlarski, J., Heimann, B. and Ortmaier, T. (2012), "Dynamics identification of kinematically redundant parallel robots using the direct search method", *Mech. Mach. Theory*, **52**(9), 277-295.

Wang, J. and Gosselin, C.M. (2004), "Kinematic analysis and design of kinematically redundant parallel mechanisms", *ASME J. Mech. Des.*, **126**(1), 109-118.

Wu, J., Wang, J.S., Li, T.M. and Wang, L.P. (2007), "Dynamic analysis of the 2-DOF planar parallel manipulator of a heavy duty hybrid machine tool", *Int. J. Adv. Manuf. Tech.*, **34**(3-4), 413-420.

Wu, J., Wang, J.S., Wang, L.P. and Li, T.M. (2009), "Dynamics and control of a planar 3-DOF parallel manipulator with actuation redundancy", *Mech. Mach. Theory*, **44**(4), 835-849.

Yi, B.J., Oh, S.R. and Suh, I.H. (1999), "Five-bar finger mechanism involving redundant actuators: analysis and its applications", *IEEE Trans. Rob. Autom.*, **15**(6), 1001-1010.

Yun, Y. and Li, Y. (2012), "Modeling and control analysis of a 3-PUPU dual compliant parallel manipulator for micro positioning and active vibration isolation", *J. Dyn. Sys. Mea. Control*, **134**(2), 021001-1-

021001-9.
Zhang, X.P., Mills, J.K. and Cleghorn, W.L. (2010), "Investigation of axial forces on dynamic properties of a flexible 3-PRR planar parallel manipulator moving with high speed", *Robotica*, **28**(4), 607-619.
Zhao, Y.J. and Gao, F. (2009), "Dynamic performance comparison of the 8PSS redundant parallel manipulator and its non-redundant counterpart- the 6PSS parallel manipulator", *Mech. Mach. Theory*, **44**(5), 991-1008.

*CC*